192 (2024) 206942

Contents lists available at ScienceDirect

Applied Catalysis O: Open

journal homepage: www.elsevier.com/locate/apcato

Carbon-dots-conjugated semiconductors for enhanced solar-driven photocatalysis

Giorgia Ferraro [a], Andrea Di Vera [b], Elena Ghedini [a], Martina Marchiori [b], Giulia Forghieri [a,*], Patrizia Canton [b], Michela Signoretto [a]

[a] Department of Molecular Sciences and Nanosystems, Ca' Foscari University of Venice and INSTM RU of Venice, via Torino 155, 30172 Venice, Italy
[b] Department of Molecular Sciences and Nanosystems, Ca' Foscari University of Venice, Stevanato Center for Electron Microscopy and CSGI RU of Venice, Via Torino 155, 30172 Venice, Italy

ARTICLE INFO

Keywords:
Photocatalysis
Solar-powered
Carbon dots
Semiconductors
Carbon dioxide

ABSTRACT

In the last decades, the rising levels of carbon dioxide (CO_2) in the atmosphere have been increasingly attributed to the global warming effect. Photocatalysis, which exploits the energy of light and abundant semiconductor materials, may represent a promising method to enable more sustainable catalytic reactions. However, the current applicability is mainly hindered by the design of materials capable of efficiently harvesting solar light to conduct photo-catalytic reactions. In this context, the conjugation of carbon dots with semiconductor materials was studied as tool to increase the visible-light sensitivity of titanium oxide (TiO_2) and barium titanate ($BaTiO_3$). The hybrid materials were tested for their photo-activity in two distinct reactions and upon the irradiation of either UV or solar light. Two different deposition methods were studied as to provide a scalable strategy to the design of versatile photocatalyst. As results, although all the prepared materials were found to be active in both UV and visible-light irradiating conditions, only carbon-modified semiconductors were able to convert CO_2 into methane upon solar light excitation. In addition, carbon-dots-$BaTiO_3$ conjugates were proposed for the first time as valid alternative to TiO_2-based photocatalysts, especially in the CO_2 photo-reduction reactions. If properly designed, carbon dots may represent a way to overcome some of the current limitations to the application of photocatalytic processes for the development solar-powered technologies.

1. Introduction

Carbon dioxide (CO_2) is the most abundant greenhouse gas emitted by human activities, accounting for 79% of global warming [1]. In the last decades, CO_2 concentration in the atmosphere has grown up to 410 ppm [2]. Different strategies, such as developing carbon-neutral fuels and energy sources, aim at reducing its concentration by means of carbon capture and storage (CCS) and carbon capture and utilization (CCU) technologies. In addition, achieving the scalable conversion of carbon dioxide as a carbon source for obtaining high-value products such as carbon monoxide, formic acid and methane, could be of high interest beside falling within the principles of the circular economy [3,4]. In particular, obtaining methane from waste could potentially play an important role in the energy transition [5]. Carbon dioxide is a non-polar, abundant, cheap, non-toxic, thermodynamically stable molecule, with high binding energies mainly relative to the C═O bond. To overcome the energy demand for CO_2 activation and to achieve net zero CO_2 emissions, new catalytic approaches such as electroreduction and photocatalysis have been currently studied [6]. While the former applies voltage to perform CO_2 reduction, which could however derive from non-renewable energy sources, photocatalysis exploits solar energy as a renewable energy source, thus resulting in a promising method to enable a more sustainable conversion [7,8]. Photocatalysis involves the use of a semiconductor, which is defined by a band structure, that is composed by a valence band and a conduction band, separated by an energy gap, usually between 0.3 and 5 eV. If the energy of irradiation is equal to or

Abbreviations: CO2, Carbon dioxide; TiO2, titanium dioxide; BaTiO3, barium titanate; CD, carbon dots; CCS, carbon capture and storage; CCU, carbon capture and utilization; TTIP, titanium tetraisopropoxide; NaOH, sodium hydroxide; FE-SEM, Scanning electron microscopy; EDX, X-ray energy dispersion; TEM, transmission electron microscopy; PL, photoluminescence; PLE, photoluminescence excitation; TCD, thermo-conductibility detector; MB, methylene blue; XRD, X-ray Diffraction; DRS, diffusion reflectance spectroscopy; FT-IR, Fourier-transform Infrared.

* Corresponding author.
E-mail address: giulia.forghieri@unive.it (G. Forghieri).

https://doi.org/10.1016/j.apcato.2024.206942
Received 18 January 2024; Received in revised form 1 May 2024; Accepted 23 May 2024
Available online 24 May 2024

greater than the band gap, there is the formation of an exciton that is composed of an electron and an empty state called hole. Electrons may move from the bulk to the surface where they are available to react with an accepting molecule, such as carbon dioxide, and performing a reducing reaction, while the hole can catalyze an oxidizing reaction, such as water into oxygen and hydrogen [9,10]. Titanium dioxide (TiO_2) is a polymorphic semiconductor composed of three different crystalline structures: rutile, anatase and brookite, with anatase being the most photo-active phase due to its higher charge mobility and therefore one of the most widely studied amongst photocatalytic materials [11,12]. Although being non-toxic, available, economic, and stable the use of TiO_2 is still limited because of its high bandgap of about 3.2 eV, which allows the absorption of radiation only in the ultraviolet region (UV), and because of its high recombination rate [13,14]. Alkaline-earth-metal perovskites show good photostability, corrosion resistance in aqueous solutions together with the band gap necessary for obtaining all the products of carbon dioxide reduction [15]. For these reasons, perovskites are currently gaining attention in photocatalytic applications. The intrinsic basicity of Barium titanate (BaTiO3) can favor the interaction with carbon dioxide – which is slightly acidic – in the photoreduction reaction [16]. Beside the promising potential of both titania and perovskites as photocatalysts, some effort is still required to improve the photoactivity efficiency and to enable these materials to fully exploit the full spectrum. Different strategies such as sensitization with visible-active dyes or polymer conjugates, doping with heteroatoms or metals, and associating the semiconductor with a co-catalyst could be applied. The latter consists in the formation of new energy levels that could promote the absorption in the visible range and the limitation of the recombination rate. Amongst the emerging photocatalytic materials, carbon dots (CD) have been already considered for organic pollutant degradation, hydrogen generation, NOx removal and organic transformations [17–20]. CDs are carbon-based spherical nanoparticles having sizes below 10 nm, high chemical stability, fluorescent properties, good photogenerated charge transfer ability, easy surface modification, biocompatibility, and low toxicity [21]. Due to their narrow band gap, CDs could be used as co-catalysts in the CO_2 photoreduction [22]. For instance, *Kulandaivalu* et al. reported the use of carbon dots supported on Cu2O for carbon dioxide photoreduction in gas phase under visible light irradiation. They obtained a high selectivity toward ethane and an improvement in the photostability of the catalytic system [23]. As a matter of fact, *Ong* et al. reported the use of carbon dots as co-catalysts to modify g-C_3N_4 (graphene carbon nitride), that has improved the adsorption of nonpolar CO_2 and has enhanced the generation of methane [24].

The synthetic methods for CDs can be divided into two categories: bottom-up and top-down approaches. Amongst the bottom-up approaches, microwave-assisted methods are environmentally friendly, cost-effective and scalable methods which apply localized and homogeneous heating, by means of microwave radiation, to decarbonize a carbon source to obtain nanoparticles [25]. In this work, carbon dots were first prepared *via* microwave-assisted method and associated as co-catalyst on a solid matrix such as $BaTiO_3$ and TiO_2 using two different deposition methods. Therefore, their potential application as co-catalysts was explored both in gas phase CO_2 photoreduction and in methylene blue photodegradation reactions, under both UV and solar irradiation.

2. Experimental

2.1. Material preparation

2.1.1. Carbon dots

Carbon dots (CD) were prepared *via* microwave-assisted method by dissolving 0.1 g of *o*-phenylenediamine (Sigma-Aldrich, ≥98%) in 20 mL of ethanol (Sigma-Aldrich, ≥99.7%), then put in a Teflon vessel which was irradiated in a microwave oven at 180 °C for 15 min. The solution was filtered with 0.22 μm WHATMAN filter papers. In order to separate larger aggregates, the solution containing the material has been centrifugated multiple times (3 times, 10,000 rpm, 5 min each) by adding small aliquots of deionized water (3 mL) in the centrifuge tube containing an ethanol solution (15 mL) of the material [26]. The precipited solid has been discarded and the purified solution was dialyzed in ethanol for 24 h with 1 kDa SPECTRA/POR membrane. Finally, the dialyzed solution was freeze-dried for 24 h.

2.1.2. Barium titanate

Barium titanate ($BaTiO_3$) was prepared *via* hydrothermal synthesis by mixing 50 mL of 0.1 M $BaCl_2{\cdot}2H_2O$ (5 mmol) (Sigma-Aldrich, ≥99%) as barium precursor and 1.5 mL of titanium tetraisopropoxide (TTIP) (Sigma-Aldrich, 97%) in a beaker. The pH value was adjusted to 12 by adding a 4 M solution of sodium hydroxide (NaOH) (Sigma-Aldrich, ≥98%) dropwise. After stirring at 300 rpm for 20 min, the solution was transferred into a Teflon vessel and kept at 180 °C in an autoclave at autogenous pressure for 8 h. The resulting mixture was left to cool down, filtered on a Gooch crucible and washed with distilled water and ethanol. The white solid sample was dried in the oven at 110 °C for 12 h.

2.1.3. Supported CDs

Titanium dioxide (TiO_2) was used in its commercial form Degussa P25 (Evonik, Italy). CD-TW and CD-BW supported samples were prepared *via* microwave-assisted solvothermal method by dissolving TiO_2 or BaTiO3 respectively, with 5 wt% *o*-phenylendiamine (Sigma-Aldrich, ≥ 98%) in ethanol and irradiating in a microwave oven as previously described. The conjugation of CD in CD-TS and CD-BS samples occurred *via* an incipient wetness impregnation procedure. In this case the CD previously synthesized in the microwave oven, were dissolved in ethanol, sonicated for 30 min and added dropwise on the scaffold in 5 wt %. Impregnated samples were dried in oven at 110 °C for 12 h. Labels and synthetic methods are reported in Table 1.

2.2. Materials characterization

Scanning electron microscopy analysis was employed to investigate carbon dots and barium titanate morphologies, using a Field Emission electron microscope (Zeiss-Sigma VP) equipped with an X-ray energy dispersion (EDX) detector (Bruker Quantax EDS). Transmission electron microscopy (TEM) was performed with a Tecnai G2 Spirit Twin equipped with a 80 kV gun to determine the morphology of the internal structure of carbon dots. Surface functional groups were investigated by FT-IR spectroscopy (Perkin Elmer Precisely Spectrum One Spectrometer). The tablets used for the measures have been composed of KBr and of a small amount of the sample. The instrument was set in a wavenumber range between 4000 and 400 cm^{-1} and with a resolution of 4 cm^{-1}. Diffuse reflectance spectroscopy (DRS) was applied to determine carbon dots interaction with light and their band gaps, operating with Cary 100 Agilent spectrometer working at room temperature in the range of 200–800 nm (UV-VIS-NIR). Spectra of all samples were converted through the Kubelka-Munk function (Eq. (1)) as proportional to the absorbance, assuming the infinitely thick samples.

$$F(R) = \frac{(1-R)^2}{2R} = \frac{K}{S} \quad (1)$$

Table 1
Sample labels by preparation method.

Sample	Material	CD synthesis	CD scaffolding
CD	Carbon dots	Microwave	/
CD-TW	CDs/TiO_2	Microwave	Incipient wetness impregnation
CD-BW	CDs/$BaTiO_3$	Microwave	Incipient wetness impregnation
CD-TS	CDs/TiO_2	Microwave	Microwave
CD-BS	CDs/$BaTiO_3$	Microwave	Microwave

where R, K, S are respectively the reflectance, absorption, and scattering coefficients of the sample [27]. To investigate the crystalline structure, X-ray Diffraction (XRD) was performed with Empyrean Bruker D8 Advanced diffractometer equipped with Cu Kα radiation (λ = 1.5418 Å), using Bragg-Brentano parafocusing geometry, PIXcel3D-Medipix3 as detector a graphite monochromator. UV-VIS spectroscopy was applied to analyze the methylene blue solutions of carbon dots, using a Cary 100 Agilent spectrometer to carry out the analysis working at room temperature in the range of 200–800 nm (UV-VIS-NIR). The emission (PL) and excitation (PLE) of the materials were investigated by means of a Jasco FP-750 spectrofluorometer equipped with a 150 W Xenon lamp (270–730 nm) as the excitation source.

2.3. Photocatalytic setup

2.3.1. Gas phase CO_2 photoreduction

CO_2 photoreduction with water vapor was carried out in a gas phase boron silicate batch reactor. A 125 W mercury UVA lamp (spectral range 315–400 nm; Helios Italquartz, GN125RZS) and a solar simulator (model number 10500; ABET technologies; 150 W Xenon arc lamp with AM 1.5G atmospheric filter) were used as light source, with an irradiance of 40 W/m^2 and 1000 W/m^2, respectively. A schematic representation of the photoreduction system is reported in Fig. 1. The gas phase reaction conditions are reported in Table 2. The blank tests were carried out in the presence of gas reagents and light for 6 h. Reaction products were analyzed by gas chromatography (Agilent 6890 Plus GC, Porapak Q column), with a thermo-conductibility detector (TCD) using Helium as gas carrier. The results are expressed in TON turn over number, according to the Eq. (2).

$$TON = \frac{\mu mol\ (product)}{g\ catalyst} \quad (2)$$

Reusability studies of the most performant catalyst were carried out under both UV and solar light, in order to assess the stability over the time. Recycles consisted in 4 cycles between which the catalyst-loaded reactor was left under He flow overnight.

2.3.2. Methylene blue photodegradation

A 125 W mercury UV lamp (spectral range 315–400 nm; HG100; Jelosil Srl) and a solar simulator were used as light sources with an irradiance equal to 40 W/m^2 and 1000 W/m^2 respectively (Table 3). Catalysts were exposed to either UV or visible light radiation into a $1 \bullet 10^{-5}$ M solution of methylene blue (MB) (Sigma-Aldrich). Aliquots of the solution were taken at regular intervals and analyzed by UV–vis spectroscopy.

Table 2
Experimental conditions for the gas-phase CO_2 photoreduction.

PARAMETERS	UV LIGHT	SOLAR LIGHT
CO_2/H_2O	13,3	13,3
Temperature (°C)	60	60
Pressure (atm)	1	1
Time (hours)	6	6
Irradiance (W/m^2)	40	1000
Catalyst mass (mg)	10	10

Table 3
Experimental conditions for liquid-phase methylene blue photodegradation.

PARAMETERS	VALUES
Temperature (°C)	25
Time (hours)	2
Irradiance UV (W/m^2)	40
Irradiance Solar (W/m^2)	1000
Catalyst concentration (g/L)	0,16
pH	6

3. Results and discussion

3.1. Structural properties

XRD analysis was applied to investigate the crystal structure of the samples.

The XRD pattern of bare carbon dots (Fig. 2a) suggested the presence of both crystalline and amorphous phases, with typical signals attributed to carbon dots. The crystalline phase denoted larger structures, whereas the amorphous one was attributed to smaller carbon particles. The crystallites dimensions were determined using Scherrer's law and ranged from 45 to 50 nm. The diffractogram of the purified CDs (Fig. 2b) shows a broad peak centered at 24°. As already reported, these type of broad signals indicates the formation nanosized crystallites, suggesting the presence of CDs materials [28].

CD-BS and CD-BW (Fig. 2 c,d) XRD patterns are characterized by the typical crystal planes: (100) 21°, (110) 31°, (111) 39°, (200) 45°, (210) 51°, (211) 56°, (220) 66°, (310) 75°, (321) 92° which were mostly attributed to the cubic phase of $BaTiO_3$ [29]. The additional peaks at 23° were attributed to $BaCO_3$ which is retained to be residual of the synthetic procedure [30]. In both Ba-based samples, the broad signal at small angles was attributed to the presence of an amorphous phase. CD-TW and CD-TS (Fig. 2 e,f) exhibited the characteristic peaks of TiO_2, that presents both rutile (110) 27°, (101) 36°, (111) 41°, (211) 54°, (220) 56°, (301) 68°, (112) 70° and anatase crystal planes (101) 25°, (004)

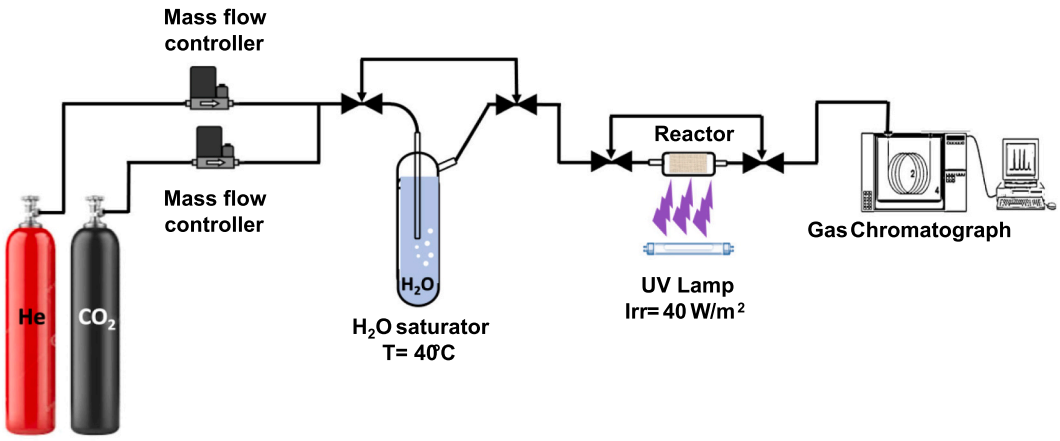

Fig. 1. CO_2 photoreduction rig.

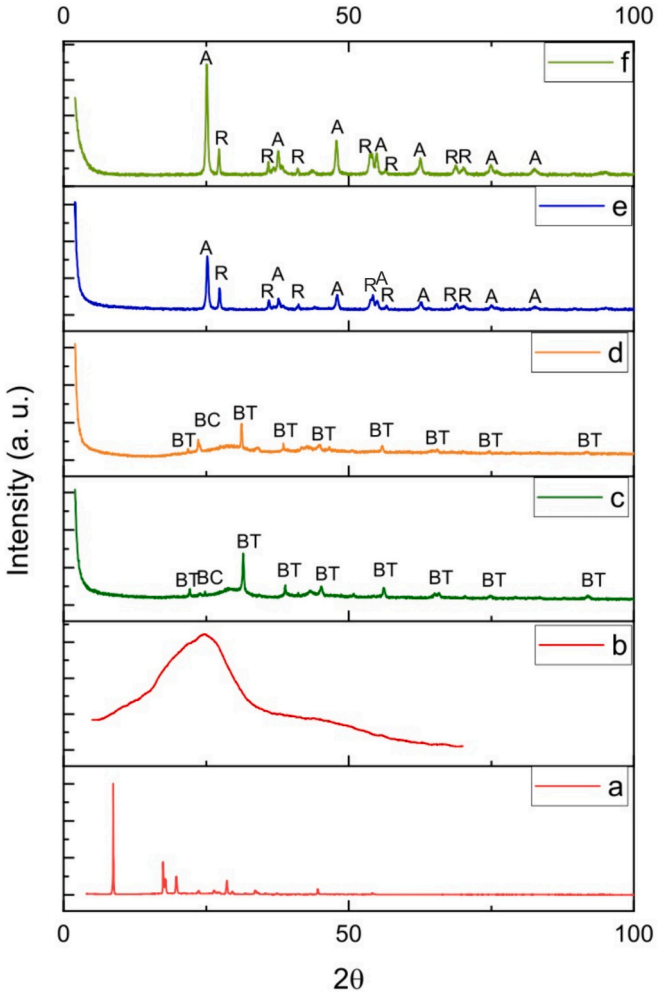

Fig. 2. XRD patterns of the catalysts: (a) CD pre-purification, (b) CD post-purification, (c) CD-BS, (d) CD-BW, (e) CD-TS, (f) CD-TW, where BT: $BaTiO_3$ crystalline phase, BC: barium carbonate phase, A: anatase phase, R: rutile phase.

37°, (200) 47°, (105) 54°, (204) 62°, (215) 75°, (224) 83° which characterize tetragonal unit cells [31]. Carbon dots peaks were not detected in any sample, either due to low concentration or to the small dimensions – or both – of carbon dots nanoparticles, leading to a weak signal not detectable by the instrument.

TEM analysis was performed to investigate bare carbon dots morphology. As reported in Fig. 3 the synthesized CDs were detected both as aggregated structures of about 200 nm (Fig. 3a) and as single nano-spheres with <10 nm size (Fig. 3b), prior to the purification step. As reported in Fig. 3a, the formation of the CDs is confirmed by means of TEM, with <10 nm size. However, the synthetic approach for the CDs leads to the formation of larger aggregates (Fig. 3b) which can be removed as already described.

Scanning electron microscopy (SEM) analysis was applied to investigate the surface morphology of the catalysts. This technique was paired with EDX to determine the distribution and the presence of defined elements in the materials.

CD-BS and CD-BW (Fig. 4a, b) showed sponge-like micro-aggregates of smaller particles with average dimension lower than 50 nm. Both samples were characterized by a homogeneous distribution of carbon on the perovskite surface, as supported by EDX analysis (Fig. S1 a,b), although CD-BW sample visibly showed fiber-like elongated structures attributed to $BaTiO_3$ that could influence the photo-activity. In addition, carbon appeared to be homogenously distributed on both CD-TS and CD-TW samples (Figs. S1c, d).

3.2. Optical properties

As reported in Fig. 5a, CD sample absorbed in the visible region, between 330 and 500 nm. This absorption peak was ascribed either to the n-π^* transition of C—O and C═O bonds, or to the functional groups on CD surface [25]. In addition, CD were found to be able to also absorb in the UV region of the spectrum. The photoluminescence (PL) of bare carbon dots was measured to determine the emission ability of the sample upon light excitation (Fig. 5b). The excitation spectrum was composed by two bands, in either UV or visible region, centered at 280 nm and 400 nm respectively, and suggesting that different types of excitations occur at the sample surface. The emission spectrum of CD was centered at 500 nm.

excitation (PLE) spectra of bare CD.

Diffused reflectance spectroscopy (DRS) was performed to confirm the absorption spectra of CD-supported samples (Fig. S2). Both CD-BS and CD-TS showed absorption both in the UV and in the visible regions, as result of the *in-situ* deposition. These same optical properties were previously observed to be related to a modification of the bandgap [32,33]. Therefore, carbon dots association to the semiconductors improved the absorption in the visible region of the spectra.

FT-IR analysis was carried out to further elucidate the role and presence of functional groups on the catalysts surface (Fig. 6). All samples exhibited a strong band at 3440 cm^{-1} related to O—H stretching. At the same wavenumber range there is also a peak related to N—H stretching of amino-groups. In CD-TS and CD-BS spectra, the peak at 1631 cm^{-1} was attributed to the bending mode H-O-H due to the physical adsorption of water. In addition, CD-TS showed C—H stretching of organic compounds, further supporting the presence of carbon as

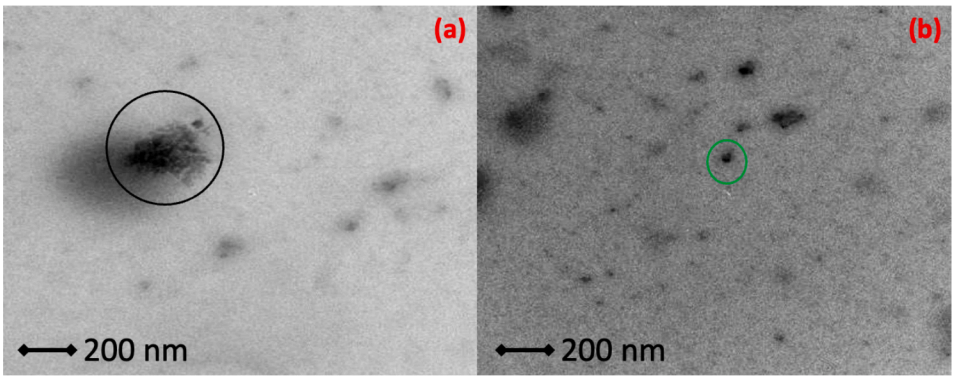

Fig. 3. TEM images of bare carbon dots: aggregated structured (black circle) and nano-spheres (green circle). (For interpretation of the references to colour in this figure legend, the reader is referred to the web version of this article.)

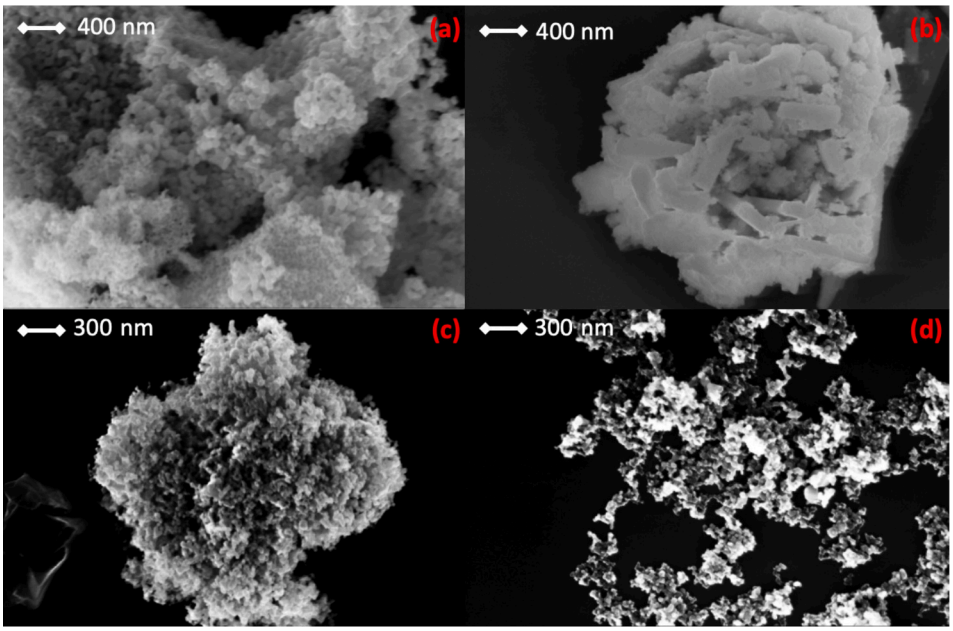

Fig. 4. SEM images: **(a)** CD-BS, **(b)** CD-BW, **(c)** CD-TS, **(d)** CD-TW.

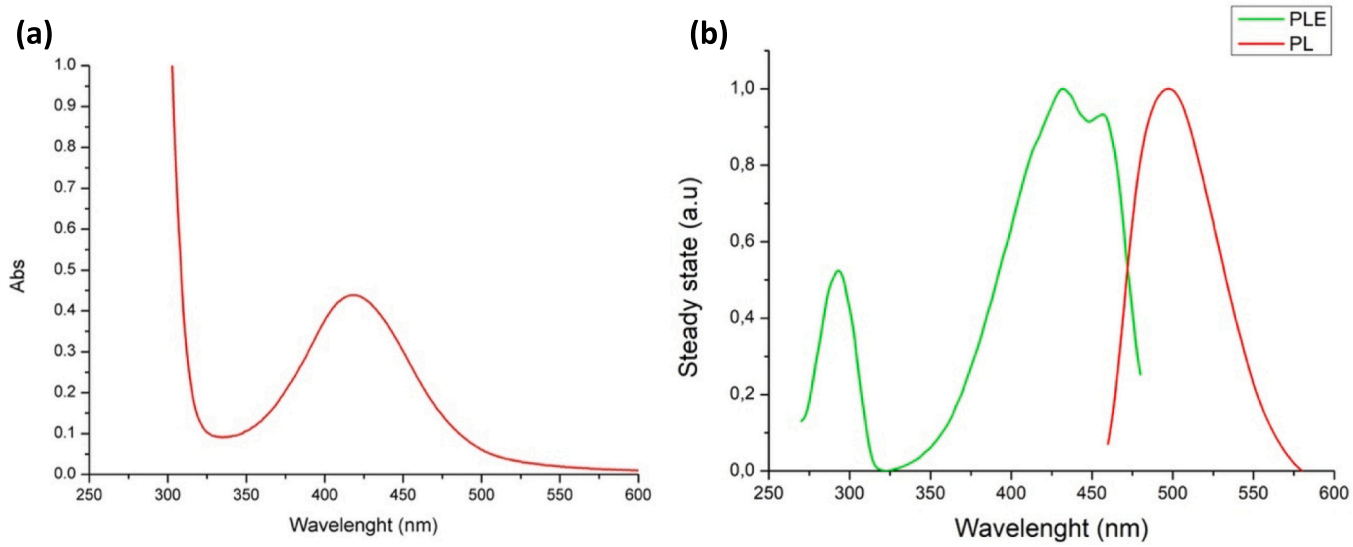

Fig. 5. **(a)** UV–vis absorption spectra of bare carbon dots. **(b)** Emission (PL) and.

suggested by SEM-EDX. The broad band at 400–700 cm^{-1} was related to bending and stretching of Ti-O-Ti of titania [34]. Similarly, CD-BS was characterized by a broad band between 800 and 400 cm^{-1} relative to Ti—O stretching of barium titanate and which was not present on bare CD spectrum. Both CD and CD-TS samples showed a more pronounced peak at 2920 cm^{-1} related to C—H stretching, compared to CD-BS sample. The peaks at 1680 cm^{-1} and at 1400 cm^{-1} attributed to the stretching vibration of C═O groups and to N—H vibration of amides respectively, were only detected in the bare CD sample. The peak at 928 cm^{-1} was attributed to C—O and C-O-C stretching of unsaturated carbon bonds formed during the carbonization process [35]. Together these C-based functional groups are thought to accelerate the separation between electrons and holes, as well as to contribute to the emission properties, being characterized large **π** conjugated system. These properties, which have been previously related to the ability of separating charge electron-hole pairs, may potentially contribute to the overall photocatalytic activity [36].

3.3. *Methylene blue photodegradation*

MB is a cationic colorant widely used in the textile industry in the dyeing of cotton, wool, and other fabrics [37]. Although MB is applied in industrial synthesis, it could cause irreparable damage to the environment due to its high toxicity and tendency to accumulate [38]. All samples were tested for methylene blue photodegradation to evaluate their photo-activity under both UV and solar light irradiation. Bare CD were active under both conditions, by recording 85% and 50% of MB degradation, respectively (Fig. 7, Table 4). The activity of bare CD under UV light irradiation was also supported by the colour shift of the solution (Fig. S3). The shift to a brownish colour observed after 90 min exposure to UV was attributed to a possible light-mediated degradation of CD and consequent precipitation of C compounds in the aqueous media [39]. Advanced oxidation processes (AOP) are often used to enable total degradation of organic molecules [40,41]. When heterogenous photocatalysts are involved, the electrons and holes in the conduction band

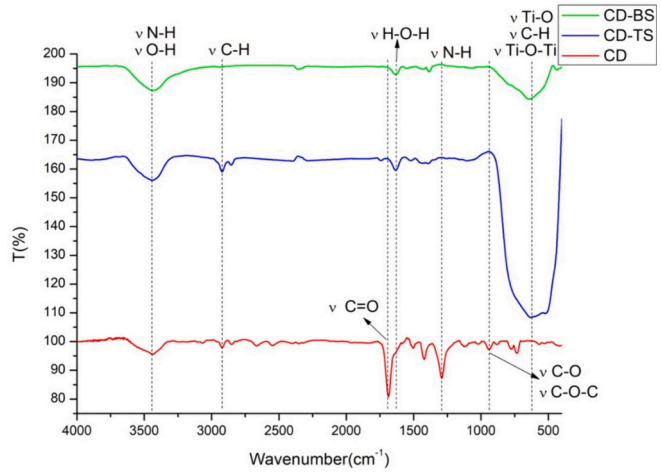

Fig. 6. FT-IR spectra of CD (black), CD-TS (blue), CD-BS (red). (For interpretation of the references to colour in this figure legend, the reader is referred to the web version of this article.)

can react with oxygen adsorbed on the surface of the catalyst to generate superoxide and hydroxyl radicals, with consequent oxidation of the target molecule *via* AOP [42]. A similar mechanism was hypothesized as responsible for the self-degradation of the catalyst. *Abbasi* et al. previously reported a photodegradation efficiency of 96% for bare carbon dots [43]. In case of CD sample, it is possible that aggregation of small particles in micrometric structures partially hindered the photo-lytic activity, by reducing the overall surface available for the reaction to occur and by promoting self-degradation due to the increased density. This effect was attributed to the reduced performance of CD sample, with respect to the values reported in literature. This was also supported by *Heng* et al., who reported that the nanoparticles aggregation could minimize the interaction with methylene blue molecules, which normally interact by aromatic and oxygen functional groups on carbon dots surface [44]. In comparison, TiO_2-based catalysts were able to completely degrade MB after 10 min UV irradiation, including both CD-TW and CD-TS samples. The activity of these samples was similar under solar irradiation, although complete MB degradation was achieved after 40 min. Conversely, both CD-BS and CD-BW showed a slower photodegradation rate compared to bare $BaTiO_3$ both under UV and solar light irradiation. Moreover, it is possible that the presence of morphology of $BaTiO_3$ material influenced negatively the photo-activity of CD-BW, as elsewhere suggested [33]. Both samples recorded a MB conversion rate lower than 20% when exposed to solar light (Table 4). Compared to another work, which reported a complete degradation of MB by NCQDs-TiO_2 catalyst only after 240 min of UV light exposure, most of the catalysts in the current study showed a complete MB degradation completely degraded after 120 min under UV light [44]. This supported positively the activity of the synthetized samples. In any case, supporting CD led to higher photodegradation efficiency than the bare CD. Apparently, while the synthetic method did not affect the photodegradation ability of CD-supported-titanium-based samples, the activity of barium titanate was affected in a less predictable way.

3.4. CO_2 photoreduction

All catalysts were tested for CO2 photoreduction, and results are reported in Fig. 8. While all catalysts were active when exposed to UV radiation, only the CD-based catalysts proved to be photo-active under solar light irradiating conditions, with the exception for bare CD. Despite being photo-active, as supported by the MB experiment, it is still possible that the energy of the band gap of CD sample was not sufficient to perform the high-energy step required to initiate of CO_2 reduction, as also suggested by the PL excitation spectra (Fig. 5b). This evidence was also noticed in the work of *Lin* et al., in which carbon dots alone showed no photoactivity in CO_2 photoreduction under UV light [45]. The decrease in the photocatalytic activity of carbon dots-conjugated semiconductors under UV light could be attributed to the competition absorption of CO_2 on the semiconductors and carbon dots surfaces. Although occurring at the expenses of the overall efficiency, the conjugation of CD with semiconductors clearly enabled the photoreduction of CO_2 under visible light irradiation. In this case carbon dots could act as light-harvesters or energy-converters, emitting light in the visible region, as supported by the PL/PLE spectra reported in Fig. 5b. Furthermore, as reported in the work of *Wang* et al., the addition of carbon dots can increase the surface distribution and the arrangement

Table 4
MB degradation percentage under both UV and solar light.

	UV MB Degradation (%)	Solar MB Degradation (%)
CD	85	50
CD-BS	100	10
CD-TS	100	100
CD-BW	100	20
CD-TW	100	100

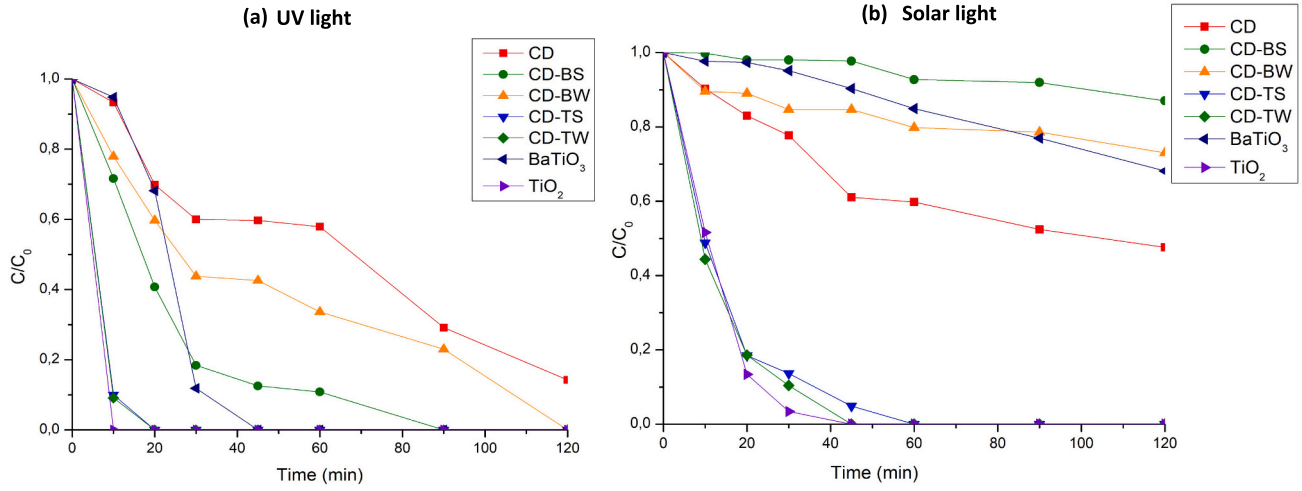

Fig. 7. Photodegradation curves of methylene blue under **(a)** UV and **(b)** solar light irradiation. (For interpretation of the references to colour in this figure legend, the reader is referred to the web version of this article.)

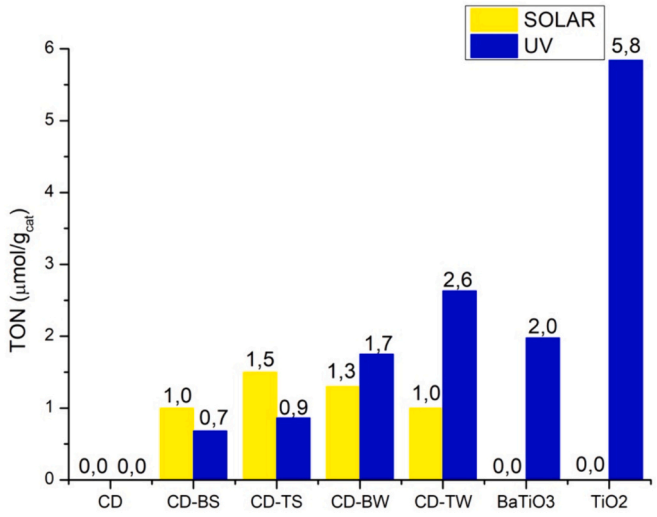

Fig. 8. Methane production under both UV (blue) and solar light (yellow). (For interpretation of the references to colour in this figure legend, the reader is referred to the web version of this article.)

of defect locations of the catalysts, delivering more active sites. In addition, the association of these nanoparticles could improve the electrical charges and distribution [46,47]. Therefore, the shape-irregular carbon-based catalysts syntetized in this work (as reported in Fig. 4 a, b, c, d) may offer a better promotion of the active sites for the absorbing reagents during the reaction. This was showed also by *Gao* et al., in which BiPdC nanostructured catalyst used for CO_2 reduction presented irregular interfaces which allowed the absorption of intermediates and accelerate electron transfer [48]. The *in-situ* deposition of CD strongly influenced the UV-mediated activity, while promoting the solar-driven conversion of CO_2 into methane, with CD-TS resulting in the highest TON value (1,5 **μ**mol/gcat). This effect was milder in the wetness-impregnated samples, which instead showed a comparable activity under both irradiating conditions. In general, titanium-based samples showed to be the most performant both under UV light and under solar light conditions. These effects on the photocatalytic activity were attributed to the CD deposition method employed. In the case of the *in-situ* synthesis of CD, surface structural modifications may result upon exposure to the synthetic conditions, thereby potentially decreasing the intrinsic photo-activity of the semiconductors. This effect is not likely to happen with incipient wetness impregnation, in which previously synthesized CD are deposited onto the surface of bare semiconductors, without exposure to potential surface-modifying conditions. In this case, reduced activity was possibly attributed to overall reduced surface availability, as above mentioned. Moreover, as reported by FT-IR analysis, the functional groups attributed to CD sample were less evident in the *in-situ* synthesized samples, namely CD-BS and CD-TS. This difference suggested that the properties of C-based structures on the surface of these samples may be different than the ones of CD-BW and CD-TW samples. On one side, it is possible that the *in-situ* deposition promoted the generation of intra-gap states, modifying the semiconductor bandgap and its light absorption capacity as reported in DRS analysis (Fig. S2), thereby enabling CO_2 conversion under visible light excitation. On the other hand, incipient wetness impregnated CD would act as a co-catalyst, thereby promoting charge exchange and enabling photo-activity in both conditions. It was suggested that conjugation of carbon dots with TiO_2 was able to slow down the recombination and improve visible-light absorption [49]. Moreover, the presence of nitrogen-containing functional groups was suggested to improve the selectivity of CO_2 photo-reduction [50]. Despite differently affecting the overall photocatalytic activity, both deposition methods had comparable effects in the promotion of photo-responsiveness of the catalysts to solar light, whereas bare $BaTiO_3$ and TiO_2 were not active. The most performant catalyst under solar light, namely CD-TS, was recycled four times in CO_2 photoreduction under both conditions, in order to study its stability over the time. The gas-chromatograms of the cycles are reported in the Supporting Information (Fig. S4, S5). As reported in Fig. 8 and in Fig. S5, under UV irradiation, the CH_4 production exhibited a decrement from the first to the second cycles, to become then constant. Under solar light, CH_4 productivity remained constant for the first two cycles, to decreased in the following ones. The possible saturation of the active sites could be responsible for the decrease in productivity, due to a decreased reactivity of the catalyst's surface [51]. (See Fig. 9.)

4. Conclusions

In this work, carbon-dots-conjugated semiconductors were tested as photocatalysts both in the photodegradation of methylene blue and in the photoreduction of CO_2, under either UV or solar irradiation. In general, supporting carbon dots to a solid matrix (such as TiO_2 or $BaTiO_3$) significantly improved the photoactivity of the latter. Moreover, conjugating CD with semiconductors, promoted CO_2 photoconversion under solar irradiation, compared to the bare samples, reaching the highest yield with CD-TS sample (1.5 **μ**mol/g_{cat}). In fact, both the bare supports and bare carbon dots were not active in these conditions. In gas phase the synthetic method did not lead to significant differences in methane production. In liquid phase, the effect was less predictable, mostly negatively affecting $BaTiO_3$-based samples. However, the different preparation of CD-conjugated samples was shown to affect the composition of functional groups and therefore the interaction with the reagents. As result, we found that the properties of the catalysts can be tailored by selecting the appropriate deposition method. Wet impregnation proved to be more effective for the design of versatile photocatalysts, active under both UV and solar light excitation, while the *in-situ* synthesis mainly favored CO_2 photoconversion activity under solar light. In addition, carbon-dots-$BaTiO_3$ conjugates were proposed for the first time as valid alternatives to TiO_2-based photocatalysts, especially in the CO_2 photo-reduction reactions. Beside the promising evidence, some effort is still required to better elucidate the reaction mechanism and the interaction between carbon dots and the semiconductor materials. If properly designed, carbon dots may represent a way to overcome some of the current limitations to the application of photocatalytic processes using solar light.

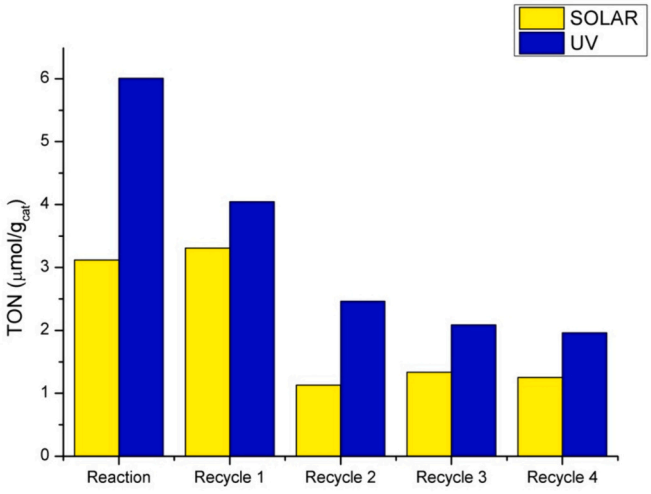

Fig. 9. CD-TS methane production under both UV (blue) and solar light (yellow) during the cycles. (For interpretation of the references to colour in this figure legend, the reader is referred to the web version of this article.)

CRediT authorship contribution statement

Giorgia Ferraro: Investigation, Writing – original draft. **Andrea Di Vera:** Data curation, Investigation, Writing – review & editing. **Elena Ghedini:** Supervision, Writing – review & editing. **Martina Marchiori:** Data curation, Investigation. **Giulia Forghieri:** Conceptualization, Methodology, Supervision, Writing – review & editing. **Patrizia Canton:** Funding acquisition, Supervision, Validation, Writing – review & editing. **Michela Signoretto:** Funding acquisition, Investigation, Supervision, Validation, Writing – review & editing.

Declaration of competing interest

The authors declare that they have no known competing financial interests or personal relationships that could have appeared to influence the work reported in this paper.

Data availability

Data will be made available on request.

Acknoledgements

"SCORE-CARIPLO" INSTM is acknowledged for funding this project.

Appendix A. Supplementary data

Supplementary data to this article can be found online at https://doi.org/10.1016/j.apcato.2024.206942.

References

[1] O. US EPA, Overview of Greenhouse Gases. https://www.epa.gov/ghgemissions/overview-greenhouse-gases, 2024 (accessed 2 July 2023).
[2] IPCC, AR6 Synthesis Report: Climate Change. https://www.ipcc.ch/report/sixth-assessment-report-cycle/, 2023.
[3] S. Dey, G.C. Dhal, D. Mohan, R. Prasad, Application of hopcalite catalyst for controlling carbon monoxide emission at cold-start emission conditions, J. Traffic Transp. Eng. Engl. Ed. 6 (2019) 419–440, https://doi.org/10.1016/j.jtte.2019.06.002.
[4] X. Chen, Y. Liu, J. Wu, Sustainable production of formic acid from biomass and carbon dioxide, Mol. Catal. 483 (2020) 110716, https://doi.org/10.1016/j.mcat.2019.110716.
[5] L. Sun, Y. Wang, N. Guan, L. Li, Methane activation and utilization: current status and future challenges, Energ. Technol. 8 (2020) 1900826, https://doi.org/10.1002/ente.201900826.
[6] IEA, International Energy Agency, IEA, 2024. https://www.iea.org/data-and-statistics (accessed 10 July 2023).
[7] X. Yang, D. Wang, Photocatalysis: from fundamental principles to materials and applications, ACS Appl. Energy Mater. 1 (2018) 6657–6693, https://doi.org/10.1021/acsaem.8b01345.
[8] I. Arora, H. Chawla, A. Chandra, S. Sagadevan, S. Garg, Advances in the strategies for enhancing the photocatalytic activity of TiO_2: Conversion from UV-light active to visible-light active photocatalyst, Inorg. Chem. Commun. 143 (2022) 109700, https://doi.org/10.1016/j.inoche.2022.109700.
[9] T.P. Nguyen, D.L.T. Nguyen, V.-H. Nguyen, T.-H. Le, D.V.N. Vo, Q.T. Trinh, S.-R. Bae, S.Y. Chae, S.Y. Kim, Q.V. Le, Recent advances in TiO_2-based Photocatalysts for reduction of CO_2 to fuels, Nanomaterials 10 (2020) 337, https://doi.org/10.3390/nano10020337.
[10] J. Ma, N. Sun, X. Zhang, N. Zhao, F. Xiao, W. Wei, Y. Sun, A short review of catalysis for CO_2 conversion, Catal. Today 148 (2009) 221–231, https://doi.org/10.1016/j.cattod.2009.08.015.
[11] A. Meng, L. Zhang, B. Cheng, J. Yu, Dual Cocatalysts in TiO_2 Photocatalysis, Adv. Mater. (2019) 1807660, https://doi.org/10.1002/adma.201807660.
[12] I. Som, M. Roy, Recent development on titania-based nanomaterial for photocatalytic CO_2 reduction: a review, J. Alloys Compd. 918 (2022) 165533, https://doi.org/10.1016/j.jallcom.2022.165533.
[13] X. Chen, H. Zhu, 3.01- catalysis by supported gold nanoparticles, in: D.L. Andrews, G.D. Scholes, G.P. Wiederrecht (Eds.), Comprehensive Nanoscience and Technology, Academic Press, Amsterdam, 2011, pp. 1–11, https://doi.org/10.1016/B978-0-12-374396-1.00095-7.
[14] V. Trevisan, A. Olivo, F. Pinna, M. Signoretto, F. Vindigni, G. Cerrato, C.L. Bianchi, C-N/TiO_2 photocatalysts: effect of co-doping on the catalytic performance under visible light, Appl. Catal. B Environ. 160–161 (2014) 152–160, https://doi.org/10.1016/j.apcatb.2014.05.015.
[15] H. Mai, D. Chen, Y. Tachibana, H. Suzuki, R. Abe, R.A. Caruso, Developing sustainable, high-performance perovskites in photocatalysis: design strategies and applications, Chem. Soc. Rev. 50 (2021) 13692–13729, https://doi.org/10.1039/D1CS00684C.
[16] P. Kanhere, Z. Chen, A review on visible light active perovskite-based Photocatalysts, Molecules 19 (2014) 19995–20022, https://doi.org/10.3390/molecules191219995.
[17] D. Saini, A.K. Garg, C. Dalal, S.R. Anand, S.K. Sonkar, A.K. Sonker, G. Westman, Visible-light-promoted photocatalytic applications of carbon dots: a review, ACS Appl. Nano Mater. 5 (2022) 3087–3109, https://doi.org/10.1021/acsanm.1c04142.
[18] K. Akbar, E. Moretti, A. Vomiero, Carbon dots for photocatalytic degradation of aqueous pollutants: recent advancements, Adv. Opt. Mater. 9 (2021) 2100532, https://doi.org/10.1002/adom.202100532.
[19] B. Li, Q. Fang, Y. Si, T. Huang, W.Q. Huang, W. Hu, A. Pan, X. Fan, G.F. Huang, Ultra-thin tubular graphitic carbon nitride-carbon dot lateral heterostructures: one-step synthesis and highly efficient catalytic hydrogen generation, Chem. Eng. J. 397 (2020) 125470, https://doi.org/10.1016/j.cej.2020.125470.
[20] J. Zhao, C. Li, X. Du, Y. Zhu, S. Li, X. Liu, C. Liang, Q. Yu, L. Huang, K. Yang, Recent Progress of carbon dots for air pollutants detection and photocatalytic removal: synthesis, Modificat., Applicati., Small. 18 (2022) 2200744, https://doi.org/10.1002/smll.202200744.
[21] J. Zhang, J. Xu, F. Tao, Interface modification of TiO_2 nanotubes by biomass-derived carbon quantum dots for enhanced photocatalytic reduction of CO_2, ACS Appl. Energy Mater. 4 (2021) 13120–13131, https://doi.org/10.1021/acsaem.1c02760.
[22] Y. Dang, B. Li, X. Feng, J. Jia, K. Li, Y. Zhang, Preparation of Iron-doped carbon dots and their application in photocatalytic reduction of carbon dioxide, ChemPhotoChem 7 (2023), https://doi.org/10.1002/cptc.202200156.
[23] T. Kulandaivalu, S. Abdul Rashid, N. Sabli, T.L. Tan, Visible light assisted photocatalytic reduction of CO_2 to ethane using CQDs/Cu_2O nanocomposite photocatalyst, Diam. Relat. Mater. 91 (2019) 64–73, https://doi.org/10.1016/j.diamond.2018.11.002.
[24] W.-J. Ong, L.-L. Tan, S.-P. Chai, S.-T. Yong, Graphene oxide as a structure-directing agent for the two-dimensional interface engineering of sandwich-like graphene–g-C_3N_4 hybrid nanostructures with enhanced visible-light photoreduction of CO_2 to methane, Chem. Commun. 51 (2015) 858–861, https://doi.org/10.1039/C4CC08996K.
[25] C. Kang, Y. Huang, H. Yang, X.F. Yan, Z.P. Chen, A review of carbon dots produced from biomass wastes, Nanomaterials 10 (2020) 2316, https://doi.org/10.3390/nano10112316.
[26] L. Deng, X. Wang, Y. Kuang, C. Wang, L. Luo, F. Wang, X. Sun, Development of hydrophilicity gradient ultracentrifugation method for photoluminescence investigation of separated non-sedimental carbon dots, Nano Res. 8 (2015) 2810–2821, https://doi.org/10.1007/s12274-015-0786-y.
[27] A.O. Murzin, A.Yu. Samsonova, C.C. Stoumpos, N.I. Selivanov, A.V. Emeline, Y. V. Kapitonov, Diffuse reflectance spectroscopy with dilution: a powerful method for halide perovskites study, Molecules 28 (2023) 350, https://doi.org/10.3390/molecules28010350.
[28] C. Xia, M. Cao, J. Xia, G. Zhou, D. Jiang, D. Zhang, J. Wang, H. Li, An ultrafast responsive and sensitive ratiometric fluorescent pH nanoprobe based on label-free dual-emission carbon dots, J. Mater. Chem. C 7 (2019) 2563, https://doi.org/10.1039/c8tc05693e.
[29] W.W. Lee, W.H. Chung, W.S. Huang, W.C. Lin, Y.R. Jiang, C.C. Chen, Photocatalytic activity and mechanism of nano-cubic barium titanate prepared by a hydrothermal method, J. Taiwan Inst. Chem. Eng. 44 (2013) 660–669, https://doi.org/10.1016/j.jtice.2013.01.005.
[30] M.C.B. del Lopez, G. Fourlaris, B. Rand, F.L. Riley, Characterization of Barium Titanate Powders:Barium Carbonate Identification, J. Am. Ceram. Soc. 82 (7) (1999) 1777–1786, https://doi.org/10.1111/j.1151-2916.1999.tb01999.
[31] H. Xi, Y. Xua, W. Zou, J. Ji, Y. Caia, H. Wan, L. Donga, Enhanced methanol selectivity of CuO/TiO_2 photocatalytic CO_2 reduction: synergistic mechanism of surface hydroxyl and low-valence copper species, J. CO2 Util. 55 (2022) 101825, https://doi.org/10.1016/j.jcou.2021.101825.
[32] G. Forghieri, D. Zanardo, E. Ghedini, F. Menegazzo, A. Giordana, G. Cerrato, A. Di Michele, G. Cruciani, M. Signoretto, Structural and functional behaviour of Ce-doped WideBandgap semiconductors for photo-catalytic applications, Catalysts 11 (2021) 1209, https://doi.org/10.3390/catal11101209.
[33] A. Virdee, I. Martin, J.Z.Y. Tan, G. Forghieri, M.M. Maroto-Valer, M. Signoretto, M. Van der Spek, J.M. Andresen, Investigation of process parameters for solar fuel production using earth-abundant materials, J. CO2 Utilizat. 75 (2023) 102568, https://doi.org/10.1016/j.jcou.2023.102568.
[34] M. Rashidzadeh, Synthesis of high-thermal stable titanium dioxide nanoparticles, Int. J. Photoenerg. 2008 (2008) 1–4, https://doi.org/10.1155/2008/245981.
[35] L. Jin, L. Zhang, X. Wu, C. Zhang, K. Wei, L. He, X. Han, H. Qiao, A.M. Asiri, K. A. Alamry, K. Zhang, Orange-red, green, and blue fluorescence carbon dots for white light emitting diodes, J. Mater. Sci. Technol. 50 (2020) 184–191, https://doi.org/10.1016/j.jmst.2020.03.020.
[36] P. Kumar, S. Dua, R. Kaur, M. Kumar, G. Bhatt, A review on advancements in carbon quantum dots and their application in photovoltaics, RSC Adv. 12 (2022) 4714–4759, https://doi.org/10.1039/D1RA08452F.
[37] R.S. Dariani, A. Esmaeili, A. Mortezaali, S. Dehghanpour, Photocatalytic reaction and degradation of methylene blue on TiO_2 nano-sized particles, Optik 127 (2016) 7143–7154, https://doi.org/10.1016/j.ijleo.2016.04.026.
[38] M. Hassanpour, H. Safardoust-Hojaghan, M. Salavati-Niasari, Degradation of methylene blue and rhodamine B as water pollutants via green synthesized Co_3O_4/

ZnO nanocomposite, J. Mol. Liq. 229 (2017) 293–299, https://doi.org/10.1016/j.molliq.2016.12.090.
[39] L. Ai, Y. Yang, B. Wang, J. Chang, Z. Tang, B. Yang, S. Lu, Insights into photoluminescence mechanisms of carbon dots: advances and perspectives, Sci. Bull. 66 (2021) 839–856, https://doi.org/10.1016/j.scib.2020.12.015.
[40] I.M. Sosnin, S. Vlassov, L.M. Dorogin, Application of polydimethylsiloxane in photocatalyst composite materials: a review, React. Funct. Polym. 158 (2021) 104781, https://doi.org/10.1016/j.reactfunctpolym.2020.104781.
[41] M.A. Rauf, S.S. Ashraf, Fundamental principles and application of heterogeneous photocatalytic degradation of dyes in solution, Chem. Eng. J. 151 (2009) 10–18, https://doi.org/10.1016/j.cej.2009.02.026.
[42] A. Houas, Photocatalytic degradation pathway of methylene blue in water, Appl. Catal. B Environ. 31 (2001) 145–157, https://doi.org/10.1016/S0926-3373(00)00276-9.
[43] A. Abbasi, M. Abushad, A. Khan, Z.U.H. Bhat, S. Hanif, M. Shakir, Bare undoped nontoxic carbon dots as a visible light photocatalyst for the degradation of methylene blue and Congo red, Carbon Trends. 10 (2023) 100238, https://doi.org/10.1016/j.cartre.2022.100238.
[44] Z.W. Heng, W.C. Chong, Y.L. Pang, L.C. Sim, C.H. Koo, Photocatalytic degradation of organic pollutants using green oil palm frond-derived carbon quantum dots/titanium dioxide as multifunctional photocatalysts under visible light radiation, Chin. J. Chem. Eng. 51 (2022) 21–34, https://doi.org/10.1016/j.cjche.2021.10.021.
[45] L.Y. Lin, S. Kavadiya, B.B. Karakocak, Y. Nie, R. Raliya, S.T. Wang, M.Y. Berezin, P. Biswas, ZnO1−x/carbon dots composite hollow spheres: facile aerosol synthesis and superior CO_2 photoreduction under UV, visible and near-infrared irradiation, Appl. Catal. B Environ. 230 (2018) 36–48, https://doi.org/10.1016/j.apcatb.2018.02.018.
[46] T. Wang, Q. Zhang, K. Lian, G. Qi, Q. Liu, L. Feng, G. Hu, J. Luo, X. Liu, Fe nanoparticles confined by multiple-heteroatom-doped carbon frameworks for aqueous Zn-air battery driving CO_2 electrolysis, J. Colloid Interface Sci. 655 (2024) 176–186, https://doi.org/10.1016/j.jcis.2023.10.157.
[47] X. Wang, S. Liu, H. Zhang, S. Zhang, G. Meng, Q. Liu, Z. Sun, J. Luo, X. Liu, Polycrystalline SnS_x nanofilm enables CO_2 electroreduction to formate with high current density, Chem. Commun. 58 (2022) 7654, https://doi.org/10.1039/d2cc01888h.
[48] S. Gao, S. Chen, Q. Liu, S. Zhang, G. Qi, J. Luo, X. Liu, Bifunctional BiPd alloy particles anchored on carbon matrix for reversible Zn−CO_2 battery, ACS Appl. Nano Mater. 5 (2022) 12387–12394, https://doi.org/10.1021/acsanm.2c02917.
[49] R.M.S. Sendão, M. Algarra, E. Ribeiro, M. Pereira, A. Gil, N. Vale, J.C.G.E. da Silva, L.P. da Silva, Carbon dots–TiO_2 nanocomposites for the enhanced visible-light driven Photodegradation of methylene blue, Adv. Sustain. Syst. 2300317 (2023) 1–15, https://doi.org/10.1002/adsu.202300317.
[50] Z. Liu, Z. Wang, S. Qing, N. Xue, S. Jia, L. Zhang, L. Li, N. Li, L. Shi, J. Chen, Improving ethane selectivity of photo-induced CO_2 reduction on carbon dots through modification of nitrogen-containing groups and graphitization, Appl. Catal. B 232 (2018) 86–92, https://doi.org/10.1016/j.apcatb.2018.03.045.
[51] Y. Chiu, T.F.M. Chang, C.Y. Chen, M. Sone, Y.J. Hsu, Mechanistic insights into Photodegradation of organic dyes using Heterostructure Photocatalysts, Catalysts 9 (2019) 430, https://doi.org/10.3390/catal9050430.